

# Effects of High-Temperature Annealing on the Microstructure and Mechanical Properties of $\beta$ -Ga<sub>2</sub>O<sub>3</sub>:Fe Crystals

D.A. Kalganov <sup>\*</sup> , D.I. Panov , V.A. Spiridonov , A.Yu. Ivanov , I.G. Smirnova ,  
D.A. Bauman 

Institute of Advanced Data Transfer Systems, ITMO University, Kronverkskiy pr., 49, lit. A, St. Petersburg, 197101, Russia

---

## Article history

Received March 06, 2026  
Accepted April 09, 2026  
Available online April 14, 2026

## Abstract

In this work, the microstructure and mechanical properties of bulk  $\beta$ -Ga<sub>2</sub>O<sub>3</sub>:Fe (0.01 mol.%) crystals were investigated using X-ray diffraction, optical transmission spectroscopy, and the ultrasonic composite oscillator technique at successive stages of two-step annealing at 1400 °C in air. Rocking curves revealed a substantial microstructural evolution, with a more complex profile envelope after 6 hours of annealing and a significant narrowing accompanied by increased reflection intensity after 12 hours. Optical transmission spectra showed an increase in transmittance below 650 nm and a decrease in the long-wavelength region. The amplitude dependences of internal friction and the effective elastic modulus were obtained and characterized. Changes in the microplastic yield point under oscillatory deformation and in the background values of these quantities were observed, indicating a reduction in the concentration of mobile defects and microstructural ordering. The effective elastic modulus measured in  $\beta$ -Ga<sub>2</sub>O<sub>3</sub>:Fe (0.01 mol.%) crystal after annealing along the  $[\bar{1}02]$  direction was found to be 186.5 GPa.

---

**Keywords:** Defects; Internal friction; Effective modulus; Gallium oxide; Ultra-wide bandgap semiconductor

## 1. INTRODUCTION

Iron-doped beta-gallium oxide ( $\beta$ -Ga<sub>2</sub>O<sub>3</sub>:Fe) represents a promising ultra-wide bandgap semiconductor material and is of considerable research interest due to its ability to exhibit highly resistive and semi-insulating properties, which are critical for passive components, buffer layers, and insulating substrates in power electronics [1–4]. In unintentionally doped  $\beta$ -Ga<sub>2</sub>O<sub>3</sub> crystals, iron ions are present in trace amounts [5]. Doping with Fe at concentrations up to 0.1 mol.% is a standard method for compensating the background *n*-type conductivity arising from residual donor impurities [6]. The incorporation of Fe ions in the crystal lattice changes the electrical and optical characteristics of bulk gallium oxide ( $\beta$ -Ga<sub>2</sub>O<sub>3</sub>) material, as well as significantly altering its defect structure, mechanical properties, and relaxation behavior [7,8]. The interaction between impurity centers and extended defects, such as

dislocations, determines the structural stability, resistance to microplastic deformation, and ultimately, the reliability of devices [9–11]. Consequently, a comprehensive assessment of the structural perfection of doped crystals is a crucial task for optimizing the technologies used in their growth and application.

Maximizing the compensating effect of the Fe dopant is possible with thermal treatment in oxygen-containing atmosphere (high-temperature annealing—HTA), which additionally involves structural ordering and passivation of defects (oxygen vacancies). Previously [8], for 0.05 mol% Fe-doped  $\beta$ -Ga<sub>2</sub>O<sub>3</sub> crystals, it was shown that HTA activates Fe ions as capture centers (traps) for carriers due to the partial transition of Fe<sup>3+</sup> to the Fe<sup>2+</sup> (electron trap) or Fe<sup>4+</sup> (hole trap) state. Moreover, oxidation from Ga<sup>1+</sup> to Ga<sup>2+</sup> occurs, reducing the number of other structural defects and promoting the relaxation of internal stresses. Thus, HTA turns out to be technological de-

\* Corresponding author: D.A. Kalganov, e-mail: [kalganov@itmo.ru](mailto:kalganov@itmo.ru)

cision, applicable to produce high-quality semi-insulating  $\beta$ -Ga<sub>2</sub>O<sub>3</sub>:Fe substrates.

Experimental methods for studying the mechanical properties of  $\beta$ -Ga<sub>2</sub>O<sub>3</sub> crystals are extremely rare, which is due to both the enormous difficulty of preparing the required set of samples and the influence of any mechanical processing on their corresponding characteristics. The study of elastic constants undertaken by Adachi et al. [12] using resonant ultrasound spectroscopy (RUS) can be considered the most significant. The resulted unusual elasticity of monoclinic  $\beta$ -Ga<sub>2</sub>O<sub>3</sub> obtained in this work is ambiguous due to the complexity of interpreting RUS data for low-symmetry lattices and the impossibility of precisely controlling the strain amplitudes. Individual effective values of Young's moduli  $E_{(100)} \sim 261$  GPa and  $E_{[010]} = 246$  GPa were also extracted from fundamental mode frequency of nanomechanical structure [13] at very high frequencies of about 50 MHz. This measurement approach does not provide useful information about the defect structure because at such high frequencies the damping of vibrations largely reflects the characteristics of the resonators' geometry rather than the intrinsic properties of the material.

The dynamic mechanical properties of  $\beta$ -Ga<sub>2</sub>O<sub>3</sub> crystals were obtained based on a combination of experiments using Kolsky-Hopkinson techniques, nanoindentation, high-speed imaging, and 3D fracture topography by the authors of Ref. [14]. These investigations revealed the classical stages in the stress-strain diagrams of the material: linear elastic stage (no cracks), nonlinear hardening stage (microcracks), and fracture failure stage (collapse of the crystal on a large scale). In the context of the current work, the distinct stages of linear elasticity and microcrack formation identified in Ref. [14] are of particular importance. A standard method for investigating the anisotropy of mechanical properties measured via angle-dependent nanoindentation of a ( $\bar{2}01$ ) oriented single crystal wafer was employed in the work [15] to establish the orientation dependence of the elastic modulus, hardness, and the plastic deformation leading to brittle fracture, all of which are governed by the crystal structure. The measured quantities in all the above-mentioned works are compared with their values evaluated from first principles, which reflect the structure of an ideal crystal. In our previous studies (see, e.g., Ref. [16]), attempts were made to measure the effective modulus at a frequency of about 100 kHz, as well as the internal friction, using the composite oscillator method.

The piezoelectric ultrasonic composite oscillator technique (PUCOT) is commonly used experimental technique for the study of microstructure, defect mobility and microplastic processes of the bulk material. It enables the measurement of internal friction (IF,  $\delta$ ) and the effective modulus ( $E$ ) at high frequencies ( $\sim 10^5$  Hz) [17,18]. At

low strain amplitude value  $E_0$  of effective modulus correspond to the value of the Young's modulus determined by the set of diagonal elastic constants for standard crystallographic directions and by the rotational transformation using direction cosines and the compliance matrix for other directions [19,20]. Concurrently, low amplitude IF data can provide reference values for the loss factor matrix by selecting modes with pure longitudinal or pure shear at high frequencies [21,22]. The amplitude dependences of  $E$  and IF characteristics indicate the interaction of mobile dislocations with both local elastic fields from point defects acting as thermally activated barriers within slip planes, and the scattering fields from the defects located outside slip planes (e.g., impurity atoms), which are overcome via athermal processes [18]. Recent PUCOT studies on gallium oxide-based solid solutions Ga<sub>2</sub>O<sub>3</sub>-Al<sub>2</sub>O<sub>3</sub> have successfully revealed the influence of aluminum ions on relaxation mechanisms and energy dissipation [23]. This approach, applied to  $\beta$ -Ga<sub>2</sub>O<sub>3</sub>:Fe crystals, would directly probe the contribution of iron ions to the dislocation pinning processes or the generation of long-range scattering fields, thereby linking fundamental defect interactions to the material's structural stability during growth and its final functional properties in devices. Furthermore, the correlation between the crystallographic orientation of the material (the direction of growth or device element fabrication) and its resultant structural-mechanical properties remains a pertinent issue of engineering science. Beta phase gallium oxide  $\beta$ -Ga<sub>2</sub>O<sub>3</sub> crystals, with its low monoclinic symmetry, exhibits pronounced anisotropy in its lattice-dependent mechanical properties and strain relaxation [12,24].

Theoretical approaches to studying the elastic and plastic properties of undoped [25,26] and modified [27,28] gallium oxide, based on first-principles calculations and molecular statics methods, are also advancing alongside the growth in computational power and the adaptation of interatomic potentials. However, the predictive application of these methods faces significant limitations related to the incorporation of realistic concentrations of impurities and defects. The data from such studies typically provide reference values for experimental quantities (nanomechanical resonators [13] and indentation techniques [15,29]) or serve as initial values for their optimization functions (RUS [12]).

The aim of this work is to investigate the structural perfection of bulk single crystals of  $\beta$ -Ga<sub>2</sub>O<sub>3</sub> doped with iron ( $\sim 0.01$  mol.%). To achieve this goal, conventional methods for characterizing the microstructure and crystal-line quality of the material were employed, based on the analysis of X-ray diffraction, optical transmission spectra. Additionally, the mechanically structure-sensitive characteristics were obtained using the PUCOT method at a high frequency ( $\sim 10^5$  Hz).

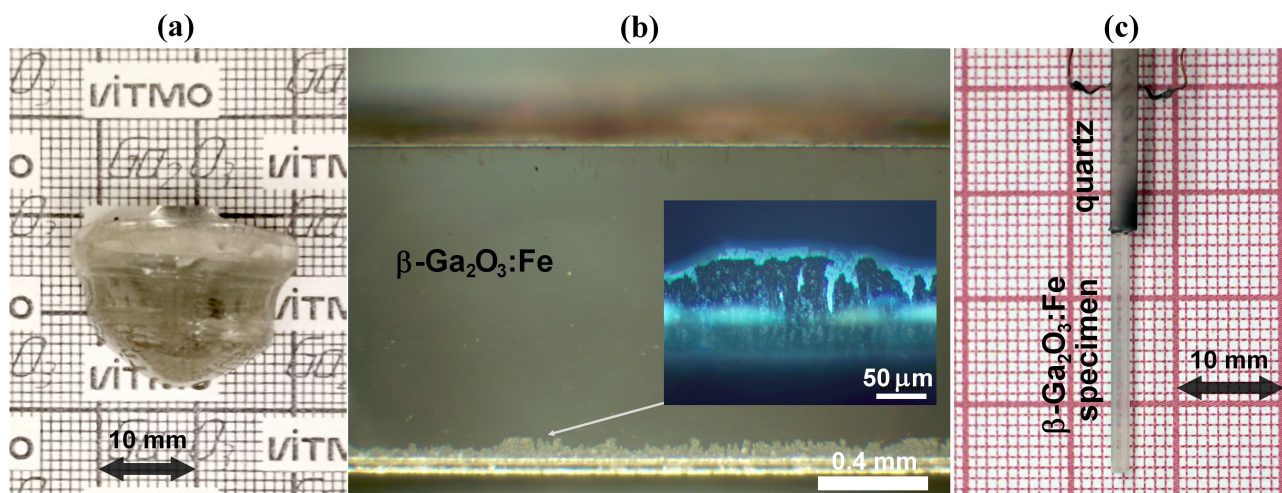


**Fig. 1.** Pristine  $\beta\text{-Ga}_2\text{O}_3\text{:Fe}$  (0.01 mol.%) material boule (a); optical microscopy image of test piece in transmitted and polarized light (inset) (b); specimen for mechanical characterization mounted on a quartz transducer (c).

## 2. MATERIALS AND TECHNIQUES

Bulk crystals of iron-doped beta-gallium oxide ( $\sim 0.01$  mol.%) were grown by the Czochralski method from the melt similar to the technology described in detail in Ref. [30]. In this work, the specimens of the material were obtained via cleaving a plate along the (100) cleavage plane of a  $\beta\text{-Ga}_2\text{O}_3\text{:Fe}$  boule (Fig. 1a) and subsequent laser cutting (for details on the cutting technique and regimes, see Ref. [31]). All studies were performed on rectangular bar-shaped specimens oriented close to the  $[\bar{1}02]$  direction (perpendicular to the crystal growth axis  $[010]$ ), with length up to 22 mm and rectangular cross-section of about  $2 \times 1.2$  mm. The crystalline quality of the cut samples was assessed using optical microscopy images (MET-5T microscope, Altami) in polarized reflected light (Fig. 1b). The density of the  $\beta\text{-Ga}_2\text{O}_3\text{:Fe}$  material, determined by standard hydrostatic weighing in an isopropanol medium, was  $\rho = 5970 \pm 11 \text{ kg/m}^3$ . The annealing conditions for the samples was selected based on the high migration energy of gallium and oxygen atoms into the corresponding vacancy sites within the sample volume, was informed by previous published data (see, e.g., Refs. [8,32]) and consisted of a two-step high-temperature treatment at  $1400^\circ\text{C}$  (6 h + 6 h) applied to the samples prepared for measurements.

Conventionally, X-ray diffraction (DRON-8 diffractometer, Bourestnik JSC) techniques are employed for analyzing crystalline quality and defect structure. Phase analysis in Bragg geometry over a wide angular range and precise rocking-curve measurements using a slit configuration enable the assessment of crystal imperfection. In particular, for  $\text{CuK}_\alpha$  radiation, the symmetric 600 reflection provides an optimal balance between penetration depth (due to extinction) and sensitivity to lattice distortions [33], making it highly effective for this purpose.

Optical transmission was investigated using unpolarized light (LAMBDA 1050, PerkinElmer) with the monochromator scanned over the range of 200 to 2000 nm in 5 nm steps, and was normalized to the level of a sample of the material with the same thickness before processing.

The composite piezoelectric oscillator method was used to obtain data on the structure-dependent characteristics of the  $\beta\text{-Ga}_2\text{O}_3\text{:Fe}$  material. A standard approach was employed, involving excitation of the fundamental longitudinal vibration mode in the frequency range of 70–140 kHz at strain amplitudes  $\varepsilon$  of  $10^{-8} - 10^{-4}$ . The values of the decrement of elastic vibrations  $\delta$  and the resonant frequency of the specimen  $f_s$  were determined analogously to the procedure described in Refs. [16,17]. The value of the effective modulus  $E$  calculated from the resonant frequency  $f_s$  by Eq. (1). The low-amplitude effective modulus  $E_0$  was determined at resonance stability strain amplitudes of  $\varepsilon = 5 \cdot 10^{-7}$ .

$$E = 4\rho(lf_s)^2, \quad (1)$$

where  $l$  is length of the sample and  $\rho$  is the density of the material under study.

The microplastic properties of the material in the standard coordinates for mechanical testing represented by the dependence of the stress  $\sigma$  on the nonlinear anelastic strain  $\varepsilon_d$ :

$$\sigma = E\varepsilon, \quad (2)$$

$$\varepsilon_d = \varepsilon \cdot (E - E_0) / E_0. \quad (3)$$

## 3. RESULTS AND DISCUSSION

In the studied specimens, regions containing macroscopic defects, including those associated with preparation by cleaving and cutting, were visualized using polarized light microscopy with crossed nicols (Fig. 1b). The largest re-

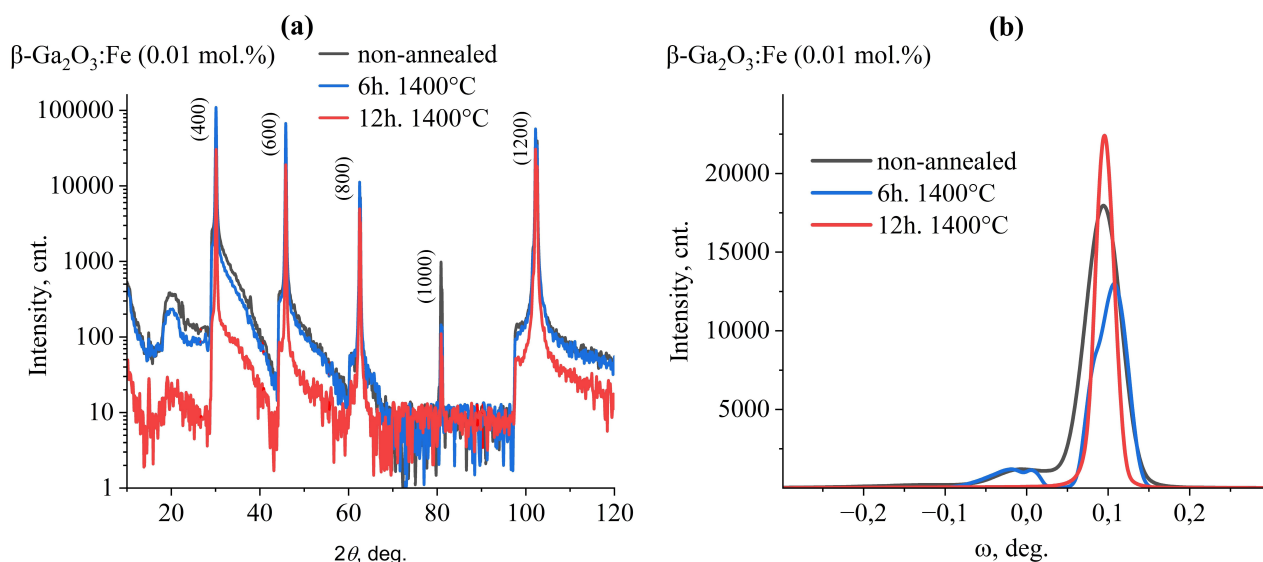


**Fig. 2.** X-ray diffraction of  $\beta\text{-Ga}_2\text{O}_3\text{:Fe}$  (0.01 mol.%) over a wide range of Bragg angles (a), and rocking curves  $\omega$  for the 600 reflection (b).

gion of damaged structure in the studied specimens was located on the cut surface and did not exceed 0.3 mm. In the central part of the crystals, which contributes most to the measured mechanical characteristics, no significant contrast caused by the presence of defects or associated internal stresses was observed.

During the X-ray diffraction study of the central region (cleaved surface) of the crystal specimens, a series of diffraction reflections corresponding to the (100) plane of the  $\beta$ -phase of gallium oxide was observed (Fig. 2a). Over a wide range of Bragg angles, the diffraction patterns of the samples before and after annealing were identical. The full width at half maximum (FWHM) of the rocking curve for the (600) reflection in the crystals before annealing was  $\text{FWHM}_0 = 2'35''$  (Fig. 2b), which is comparable to the data for undoped  $\beta\text{-Ga}_2\text{O}_3$  crystals grown under the same conditions and studied previously. After 6 hours of thermal processing, the estimated  $\text{FWHM}_{6h} = 2'16''$ . At the same time, a complication is observed in the envelope of the rocking curve, which is characterized by a large number of constituent components. After prolonged 12 hour annealing, the rocking curve qualitatively simplifies, accompanied by an increase in reflection intensity and a narrowing of the  $\text{FWHM}_{12h} = 1'23''$ , indicating a high degree of structural relaxation and a significant improvement in the crystalline quality of the material.

The optical spectroscopy results showed a substantial rearrangement of the transmittance in the visible and long-wavelength ranges as a result of the two-step annealing, with its value increasing below 650 nm and decreasing above it (Fig. 3). The difference in transmittance between the samples annealed for 6 and 12 hours was not substantial, although it maintained the trend of relative changes. Previously [8], a probable link was demonstrated between

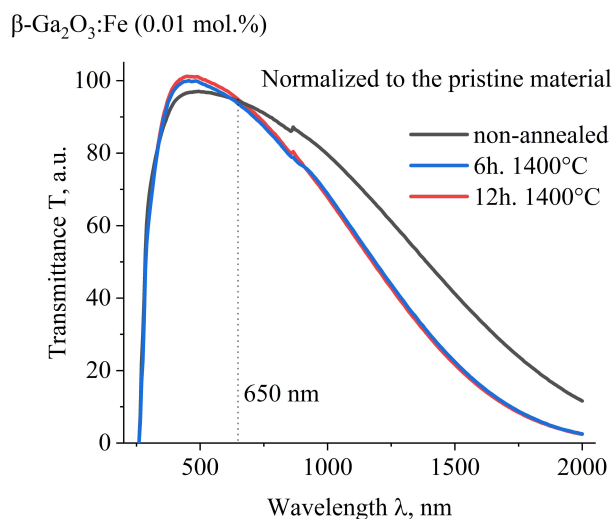


**Fig. 3.** Optical transmittance spectra of  $\beta\text{-Ga}_2\text{O}_3\text{:Fe}$  (0.01 mol.%) crystal before and after two-step annealing in air.

the decrease in transmittance in the visible region upon annealing and an indirect increase in capture centers, which absorb photons via electrons trapped at defect levels. The increase in transmittance in the range from the absorption edge to 650 nm after annealing at 1400 °C for 12 h in an iron-doped (0.01 mol.%)  $\beta\text{-Ga}_2\text{O}_3$  crystal may be attributed to several interrelated processes, which to a greater extent involve the redistribution of both residual impurities and intrinsic defects (gallium and oxygen vacancies, Si) of pristine  $\beta\text{-Ga}_2\text{O}_3$ , as previously observed for undoped crystals in Refs [16,34], and, to a lesser extent (proportionally to the doping fraction), changes in the charge state of Fe and a decrease in optically active centers.

Using the piezoelectric ultrasonic composite oscillator technique, the values of the damping decrement  $\delta$  of

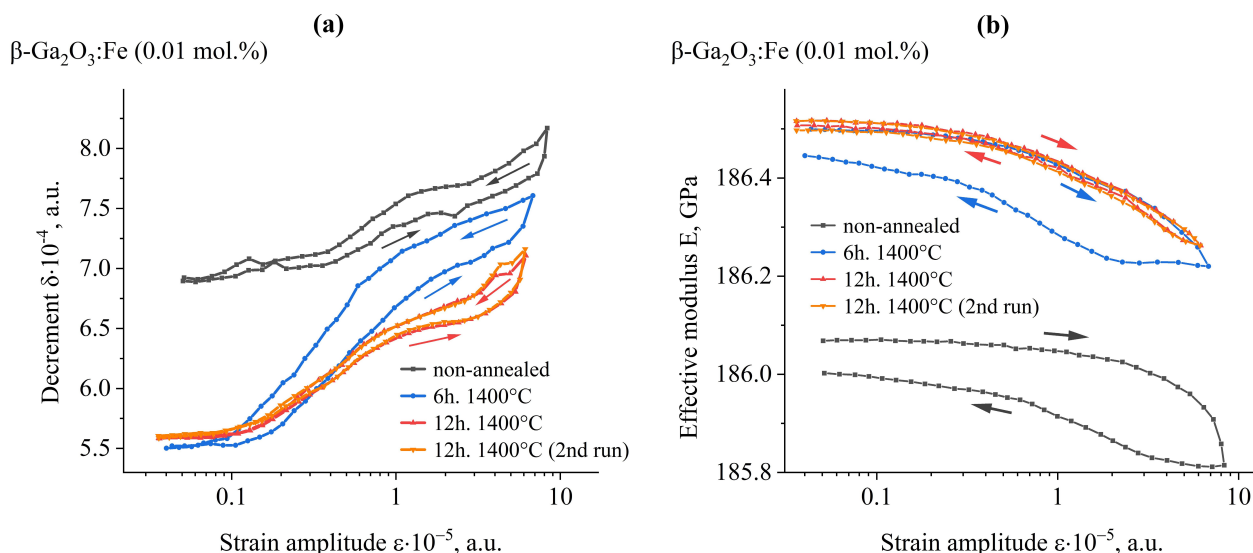


**Fig. 4.** Mechanical characteristics of  $\beta\text{-Ga}_2\text{O}_3\text{:Fe}$  (0.01 mol.%): amplitude dependences of the damping decrement  $\delta$  of elastic vibrations (a) and of the effective elastic modulus  $E$  (b). Arrows indicate the forward and reverse run in increasing and decreasing strain amplitude.

elastic vibrations (IF) and the effective modulus  $E$  were obtained for the  $\beta\text{-Ga}_2\text{O}_3\text{:Fe}$  (0.01 mol.%) single-crystalline material at various annealing stages, with the strain amplitude varied over the range of  $10^{-7}$  to  $10^{-4}$ . Typical curves of the amplitude dependences of these quantities  $\delta(\varepsilon)$  and  $E(\varepsilon)$  are shown in Fig. 4. The internal friction curves for the studied samples (Fig. 4a) exhibit a pronounced amplitude dependence above  $\varepsilon_y = 10^{-6}$  (the microplastic yield point) and a small positive hysteresis. Moreover, the amplitude dependence and the boundaries of  $\varepsilon_y$  are more pronounced in the samples after annealing. The values of background internal friction, which characterize the number of various mobile defects in the material, noticeably decrease after annealing, indicating a reduction in the total number of microstructural defects (coagulation into macroscopic defects and out-diffusion to the surface) or their mutual immobilization. The shape of the amplitude dependence changes sequentially; however, the hysteresis area (between the forward and reverse sweeps) is larger at the intermediate stage, which may indicate the complex nature of the processes that variously affect the mobility of defects (dislocations, impurity atoms, and vacancies) during annealing. For the selected excitation type (quartz resonator) and maximum amplitudes  $\varepsilon_{\max} \sim 10^{-4}$ , the damping does not exhibit saturation or a significant change in the amplitude dependence. The amplitude dependences of the effective elastic modulus  $E(\varepsilon)$  show conventional behavior during the oscillatory deformation of the sample (Fig. 4b). The decrease in values  $E$  upon the reverse sweep (negative hysteresis) is associated with the vibration of dislocation segments in the material. Upon annealing, the (elastic) stiffness of the material increases and the hysteresis area sharply decreases. In comparison with

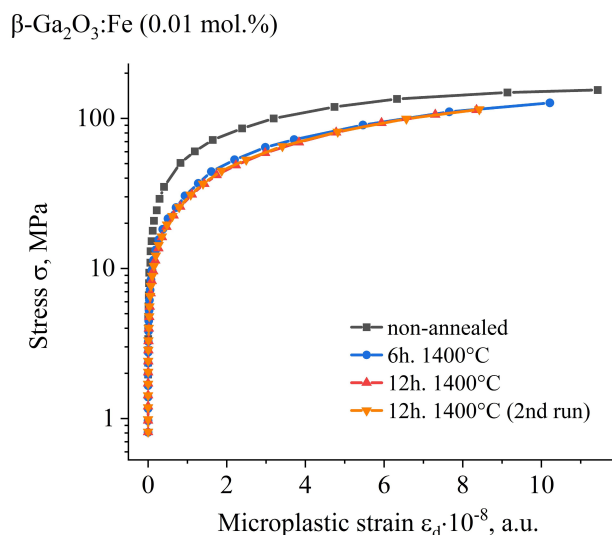


**Fig. 5.** The acoustic deformation diagram of  $\beta\text{-Ga}_2\text{O}_3\text{:Fe}$  (0.01 mol.%) in the stress-microplastic strain coordinates.

macroscopic brittle-plastic deformation [14], the present work describes the initial stage of dislocation mobility. The acoustic deformation diagram in the coordinates of stress versus microplastic strain  $\sigma(\varepsilon_d)$  given by Eqs. (2,3) for the studied samples is shown in Figure 5. The microplastic yield point in terms of strain amplitude is governed by the local interaction of dislocations with point defects and is approximately 4 orders of magnitude lower than the yield strength caused by the nucleation and growth of microcracks, and dislocation slip at larger scales.

The initial (background) values of the effective elastic modulus  $E$  are in agreement with known literature data. Thus, for  $E_{12h} = 186.5 \pm 0.2$  GPa value  $E_{[102]}$  lies between the values  $E_{[100]}$  and  $E_{[001]}$  and is much lower than

the value in the crystallographic other directions with higher ions density  $E_{[010]}$ . Using the crystal lattice anisotropy based procedure given in Ref. [26], one can obtain  $E_{[010]} = 254$  GPa for the crystals  $\beta$ -Ga<sub>2</sub>O<sub>3</sub>:Fe (0.01 mol.%) under study.

#### 4. CONCLUSIONS

In the present work, an attempt was made to ensure the maximum correspondence between the properties of the bar-shaped specimen and those of the pristine crystalline material, as confirmed by optical microscopy and X-ray diffraction data (Figs. 1 and 2). The  $\beta$ -Ga<sub>2</sub>O<sub>3</sub>:Fe (0.01 mol.%) single-crystalline material studied in this work exhibited complex behavior in terms of microstructural evolution and changes in mechanical properties upon high-temperature 1400 °C (6 h + 6 h) annealing in an oxygen-containing atmosphere. X-ray diffraction data indicate a high degree of crystallinity, and the rocking curves reflect a stepwise evolution of the microstructure with relatively unchanged parameter (Bragg angle of 600) of the main crystalline blocks, but with a decrease in the number of misoriented or dilated ones. The complex behavior of optical transmittance (Fig. 3) upon annealing reproduces that previously observed for undoped crystals [16], except for the low transmittance in the long-wavelength region, which is associated with the semi-insulating properties of the material due to Fe<sup>3+</sup> traps [8]. The measured values of the effective elastic modulus are lower than those previously obtained by us for undoped gallium oxide in the [010] direction [16] and are consistent, taking into account the orientation, with other known data.

The obtained result, based on the analysis of the amplitude-dependent parts of internal friction and the modulus  $E$ , makes it possible to optimize the commonly used annealing procedure for  $\beta$ -Ga<sub>2</sub>O<sub>3</sub> wafers after various types of processing. Furthermore, the data on the background decrement  $\delta$  and the modulus  $E$  can be used for calculations involving optimization of the difference between reference (first-principles) and experimental (PUCOT and RUS) values of elastic constants, loss factor and engineering moduli.

#### ACKNOWLEDGEMENTS

The authors are grateful to Professor Alexey Romanov for insightful discussion and valuable suggestions.

#### FUNDING

This work was supported by the Ministry of Science and Higher Education of the Russian Federation, project no. FSER-2025-0005.

#### REFERENCES

- [1] Y. Du, C. Zhang, S. Cui, G. Li, N. Tang, B. Shen, J. Xu, H. Tang, L. Zhao. Iron-doped  $\beta$ -Ga<sub>2</sub>O<sub>3</sub> single crystal: the iron occupying site and optical properties. *CrystEngComm*, 2025, vol. 27, no. 15, pp. 2392–2400.
- [2] K.M. Dowling, B. Chatterjee, S. Ghandiparsi, Q. Shao, J. Varley, J.D. Schneider, C. Chapin, M.S. Gottlieb, L. Leos, M. Sword, S. Harrison, L. Voss. Evaluation of Fe- $\beta$ Ga<sub>2</sub>O<sub>3</sub> for photoconductive semiconductor switching. *IEEE Trans. Electron Devices*, 2024, vol. 71, no. 3, pp. 1535–1540.
- [3] R.A. Babunts, A.S. Gurin, E.V. Edinach, Yu.A. Uspenskaya, P.G. Baranov. Features of the iron charge states in semi-insulating  $\beta$ -Ga<sub>2</sub>O<sub>3</sub>:Fe identified by high-frequency electron paramagnetic resonance. *Tech. Phys. Lett.*, 2023, vol. 49, no. 11, pp. 12–14.
- [4] M. Higashiwaki, K. Sasaki, H. Murakami, Y. Kumagai, A. Koukitu, A. Kuramata, T. Masui, S. Yamakoshi. Recent progress in Ga<sub>2</sub>O<sub>3</sub> power devices. *Semicond. Sci. Technol.*, 2016, vol. 31, no. 3, art. no. 034001.
- [5] R.A. Babunts, A.S. Gurin, E.V. Edinach, H.-J. Drouhin, V.I. Safarov, P.G. Baranov. Non-Kramers iron  $S = 2$  ions in  $\beta$ -Ga<sub>2</sub>O<sub>3</sub> crystals: High-frequency low-temperature EPR study. *J. Appl. Phys.*, 2022, vol. 132, no. 15, art. no. 155703.
- [6] A. Kuramata, K. Koshi, S. Watanabe, Y. Yamaoka, T. Masui, S. Yamakoshi. Bulk crystal growth of Ga<sub>2</sub>O<sub>3</sub>. *Proc. SPIE 10533, Oxide-based Materials and Devices IX*, 2018, art. no. 105330E.
- [7] J.P. Remeika. GaFeO<sub>3</sub>: a ferromagnetic-piezoelectric compound. *J. Appl. Phys.*, 1960, vol. 31, no. 5, pp. S263–S264.
- [8] N. Zhang, H. Liu, Q. Sai, C. Shao, C. Xia, L. Wan, Z.C. Feng, H.F. Mohamed. Structural and electronic characteristics of Fe-doped  $\beta$ -Ga<sub>2</sub>O<sub>3</sub> single crystals and the annealing effects. *J. Mater. Sci.*, 2021, vol. 56, no. 23, pp. 13178–13189.
- [9] Y. Wang, J. Su, Z. Lin, J. Zhang, J. Chang, Y. Hao. Recent progress on the effects of impurities and defects on the properties of Ga<sub>2</sub>O<sub>3</sub>. *J. Mater. Chem. C*, 2022, vol. 10, no. 37, pp. 13395–13436.
- [10] M. Higashiwaki, A. Kuramata, H. Murakami, Y. Kumagai. State-of-the-art technologies of gallium oxide power devices. *J. Phys. D: Appl. Phys.*, 2017, vol. 50, no. 33, art. no. 333002.
- [11] N.A. Mahadik, M.J. Tadjer, P.L. Bonanno, K.D. Hobart, R.E. Stahlbush, T.J. Anderson, A. Kuramata. High-resolution dislocation imaging and micro-structural analysis of HVPE- $\beta$ -Ga<sub>2</sub>O<sub>3</sub> films using monochromatic synchrotron topography. *APL Mater.*, 2019, vol. 7, no. 2, art. no. 022513.
- [12] K. Adachi, H. Ogi, N. Takeuchi, N. Nakamura, H. Watanabe, T. Ito, Y. Ozaki. Unusual elasticity of monoclinic  $\beta$ -Ga<sub>2</sub>O<sub>3</sub>. *J. Appl. Phys.*, 2018, vol. 124, no. 8, art. no. 085102.
- [13] X.Q. Zheng, H. Zhao, Z. Jia, X. Tao, P.X. Feng. Young's modulus and corresponding orientation in  $\beta$ -Ga<sub>2</sub>O<sub>3</sub> thin films resolved by nanomechanical resonators. *Appl. Phys. Lett.*, 2021, vol. 119, no. 1, art. no. 013505.
- [14] J.Q. Zhang, H. Zhou, W. Jiang, S.X. Hu, X.P. Ren, C.W. Zhang. Investigation of dynamic mechanical properties and constitutive model of (010) plane of gallium oxide crystals under shock loading. *Ceram. Int.*, 2022, vol. 48, no. 19, pp. 27823–27835.

- [15] Y. Yao, Y. Sugawara, K. Sasaki, A. Kuramata, Y. Ishikawa. Anisotropic mechanical properties of  $\beta$ -Ga<sub>2</sub>O<sub>3</sub> single-crystal measured via angle-dependent nanoindentation using a Berkovich indenter. *J. Appl. Phys.*, 2023, vol. 134, no. 21, art. no. 215106.
- [16] V.V. Kaminskii, D.I. Panov, V.A. Spiridonov, D.A. Bauman, D.A. Kalganov, M.P. Scheglov, A.E. Romanov. Effect of high-temperature annealing on the internal friction and optical transmittance of single crystal gallium oxide. *Mater. Phys. Mech.*, 2024, vol. 52, no. 5, pp. 48–54.
- [17] S. Kustov, S. Golyandin, A. Ichino, G. Gremaud. A new design of automated piezoelectric composite oscillator technique. *Mater. Sci. Eng. A*, 2006, vol. 442, no. 1–2, pp. 532–537.
- [18] G. Gremaud, S. Kustov. Theory of dislocation-solute atom interactions in solid solutions and related nonlinear anelasticity. *Phys. Rev. B*, 1999, vol. 60, no. 13, pp. 9353–9366.
- [19] A. Wolfenden, M.R. Harmouche. Elastic constants of silver as a function of temperature. *J. Mater. Sci.*, 1993, vol. 28, no. 4, pp. 1015–1018.
- [20] S. Kustov, J. Miguez Obrero, X. Wang, D. Damjanovic, E.K. Salje. Phase transitions in the ferroelectric relaxor (1-x)Pb(Mg<sub>1/3</sub>Nb<sub>2/3</sub>)O<sub>3-x</sub>PbTiO<sub>3</sub> close to the morphotropic phase boundary. *Phys. Rev. Mater.*, 2022, vol. 6, no. 12, art. no. 124414.
- [21] M. Xie, Q. Huan, F. Li. Quick and repeatable shear modulus measurement based on torsional resonance using a piezoelectric torsional transducer. *Ultrasonics*, 2020, vol. 103, art. no. 106101.
- [22] Z.H. Wu, X.P. He, H. Zheng, X.M. Zhu. An analysis of high-frequency dynamic mechanical parameters based on the design of transducer. *J. Yunnan Univ. Nat. Sci. Ed.*, 2022, vol. 44, no. 3, pp. 569–575 [in Chinese].
- [23] D.A. Kalganov, D.A. Bauman, D.Yu. Panov, V.A. Spiridonov, A.Yu. Ivanov, A.E. Romanov. Amplitude-dependent internal friction and modulus of elasticity in single crystal of Ga<sub>2</sub>O<sub>3</sub>-Al<sub>2</sub>O<sub>3</sub> solid solution. *Phys. Solid State*, 2025, vol. 67, no. 10, pp. 1930–1935.
- [24] H. Nishinaka, Y. Kajita, S. Hosaka, H. Miyake. Composition analysis of  $\beta$ -(In<sub>x</sub>Ga<sub>1-x</sub>)<sub>2</sub>O<sub>3</sub> thin films coherently grown on (010)  $\beta$ -Ga<sub>2</sub>O<sub>3</sub> via mist CVD. *Sci. Technol. Adv. Mater.*, 2024, vol. 25, no. 1, art. no. 2414733.
- [25] J. Furthmüller, F. Bechstedt. Quasiparticle bands and spectra of Ga<sub>2</sub>O<sub>3</sub> polymorphs. *Phys. Rev. B*, 2016, vol. 93, no. 11, art. no. 115204.
- [26] S. Poncé, F. Giustino. Structural, electronic, elastic, power, and transport properties of  $\beta$ -Ga<sub>2</sub>O<sub>3</sub> from first principles. *Phys. Rev. Research*, 2020, vol. 2, no. 3, art. no. 033102.
- [27] E. Welch, P. Borges, L. Scolfaro. Hybrid density functional theory study of substitutional Gd in  $\beta$ -Ga<sub>2</sub>O<sub>3</sub>. *Physica B*, 2023, vol. 651, art. no. 414558.
- [28] M.D. Ganji, H. Ko. Engineering multifunctionality in gallium oxide: unveiling novel structural, electronic, and opto-mechanical attributes of gadolinium-doped  $\beta$ -Ga<sub>2</sub>O<sub>3</sub> through advanced first-principles design. *RSC Adv.*, 2025, vol. 15, no. 49, pp. 41677–41690.
- [29] G. Chen, Z. Ni, D. Zheng, W. Lv. Micromechanical properties of  $\beta$ -Ga<sub>2</sub>O<sub>3</sub> single crystal by instrumented indentation and scratch tests. *ECS J. Solid State Sci. Technol.*, 2026, vol. 15, no. 3, art. no. 034002.
- [30] D.A. Bauman, D.I. Panov, V.A. Spiridonov, A.Yu. Ivanov, P.A. Bogdanov, W.V. Lundin, E.Yu. Lundina, A.F. Tsatsulnikov, M.V. Tokarev, B.Y. Ber, S.S. Rachkov, D.Yu. Kazantsev, P.N. Brunkov, A.E. Romanov. Control of iron doping during the growth of bulk gallium oxide crystals by the Czochralski method. *J. Vac. Sci. Technol. A*, 2025, vol. 43, no. 4, art. no. 042804.
- [31] D.I. Panov, V.A. Spiridonov, O.S. Vasilev, P.A. Bogdanov, D.A. Bauman, A.E. Romanov. Laser processing of gallium oxide crystals in the preparation of samples for microelectronics. *Rev. Adv. Mater. Technol.*, 2025, vol. 7, no. 3, pp. 198–202.
- [32] Y. Yuan, W. Hao, W. Mu, Z. Wang, X. Chen, Q. Liu, G. Xu, C. Wang, H. Zhou, Y. Zou, X. Zhao, Z. Jia, J. Ye, J. Zhang, S. Long, X. Tao, R. Zhang, Y. Hao. Toward emerging gallium oxide semiconductors: A roadmap. *Fundam. Res.*, 2021, vol. 1, no. 6, pp. 697–716.
- [33] B.K. Tanner, D.K. Bowen (Eds.). *Characterization of Crystal Growth Defects by X-Ray Methods*. Springer New York, NY, 2013, 589 p.
- [34] V.A. Spiridonov, D.I. Panov, A.Yu. Ivanov, D.A. Bauman, A.E. Romanov. The effect of high-temperature annealing on the properties of bulk  $\beta$ -Ga<sub>2</sub>O<sub>3</sub> obtained in different growth atmospheres. *Mater. Phys. Mech.*, 2024, vol. 52, no. 3, pp. 80–85.

УДК 548.4:534.631:620.192.63

## **Влияние высокотемпературного отжига на микроструктуру и механические свойства кристаллов $\beta$ -Ga<sub>2</sub>O<sub>3</sub>:Fe**

**Д.А. Калганов, Д.Ю. Панов, В.А. Спиридонов, А.Ю. Иванов, И.Г. Смирнова,  
Д.А. Бауман**

Институт перспективных систем передачи данных, Университет ИТМО, Кронверкский пр., 49, литер А, Санкт-Петербург, 197101, Россия

**Аннотация.** Микроструктура и механические свойства легированных объёмных кристаллов  $\beta$ -Ga<sub>2</sub>O<sub>3</sub>:Fe (0.01 мол.%) исследованы с использованием рентгеновской дифракции, оптической спектроскопии пропускания и метода составного пьезоэлектрического осциллятора последовательно на двух стадиях отжига 1400 °С в атмосфере воздуха. Кривые качания показали существенную эволюцию микроструктуры с усложнением составляющих профиля после 6 часов отжига и значительном сужением и увеличением интенсивности основного максимума после 12 часов. Оптическое пропускание возросло в области длин волн меньше 650 нм и уменьшилось для длинноволновой. Были получены и охарактеризованы амплитудные зависимости внутреннего трения и эффективного модуля упругости. Показано изменение предела микропластичности при колебательной деформации и изменение фоновых значений этих величин, что указывает на уменьшение концентрации подвижных дефектов и структурное упорядочение в результате высокотемпературного отжига. Эффективный модуль упругости, измеренный вдоль направления  $[\bar{1}02]$  кристаллов  $\beta$ -Ga<sub>2</sub>O<sub>3</sub>:Fe (0.01 мол.%) после отжига, составил 186,5 ГПа.

*Ключевые слова:* дефекты; внутреннее трение; эффективный модуль; оксид галлия; сверхширокозонный полупроводник